Degradation of Silicon AC-coupled Microstrip Detectors Induced by Radiation

N. Bacchetta[1$], D. Bisello[1,2], C. Canali[3], P.G. Fuochi[4], Yu. Gotra[1*], A. Paccagnella[1,5] and G. Verzellesi[1,5]

[1]INFN, Sezione di Padova, via Marzolo 8, 35131 Padova, Italy

[2]Dipartimento di Fisica, Università di Padova, via Marzolo 8, 35131 Padova, Italy

[3]Facoltà di Ingegneria, Università di Modena, via Campi 213, 41100 Modena, Italy

[4]CNR-FRAE, via de Castagnoli 1, 40126 Bologna, Italy

[5]Dipartimento di Elettronica e Informatica, Università di Padova, via Gradenigo 6a, 35131 Padova, Italy

Abstract

Results are presented showing the radiation response of AC-coupled FOXFET biased microstrip detectors and related test patterns to be used in the microvertex detector of the CDF experiment at Fermi National Laboratory. Radiation tolerance of detectors to gamma and proton irradiation has been tested and the radiation induced variations of the DC electrical parameters have been analysed. Long term post-irradiation behaviour of detector characteristics have been studied, and the relevant room temperature annealing phenomena have been discussed.

I. Introduction

In the FOXFET biased microstrip detectors used for the CDF experiment, microstrip bias is achieved by using an FET with gate and drain contacts both common to all the strips [1]. The FET features a thick Field OXide (1 μm) under the gate metal, from which the FOXFET acronym derives. Such a chip design could in principle expose the detector performance to all the radiation induced instabilities and degradation problems affecting the MOS devices [2, 3]. These effects are well known to depend on many factors: internal parameters (oxide thickness and quality, layout and processing characteristics) and external parameters during irradiation (dose rate; temperature; magnitude, polarity and frequency of bias), and final results cannot be forecasted in advance.

In this paper we present the main γ and proton radiation effects measured on the FOXFET biased detectors and test patterns, also discussing the implications of these results for detector operation. For sake of simplicity, devices have been kept unbiased during irradiation and during the subsequent post-irradiation long term storage. The bias dependence of the observed effects is currently under investigation.

II. Devices and Experimental Procedure

In this work we have used 4 inches <111> n-type silicon wafers supplied by Wacker, with electrical resistivity ρ>4 kΩcm, corresponding to a nominal doping level $N_d \leq 10^{12}cm^{-3}$. FOXFET biased microstrip detectors have been fabricated by Micron Semiconductor, Ltd. (UK), following the schematic layout and cross-section reported in Fig. 1, where the detector region close to the FOXFET is shown.

Microstrip detectors feature 256 or 384 p^+-implanted strips 12 μm wide, with a pitch of 60 μm and connections for both DC and AC signal readout. AC coupling is achieved by using MOS capacitors fabricated over the strips. FOXFET channel length is 6 μm and gate oxide thickness is 1 μm, while strip oxide is 0.2 μm thick. Gate and strip oxides were grown at different fabrication steps, both of them through a steam process.

($) Permanent address: University of New Mexico, Albuquerque, NM 87131-1156, USA

(*) On leave from Joint Institute for Nuclear Research, Dubna, P.O. Box 79, Head Post Office, 101000 Moscow, Russia

Test patterns (TP) fabricated with the detector process on the same wafers of detectors (D) feature a 1 cm^2 MOS capacitor with 1 μm thick gate oxide, a FOXFET with channel dimensions W/L of 10/5 μm, and a 1 cm^2 area p^+-n junction with a p^+ guard ring.

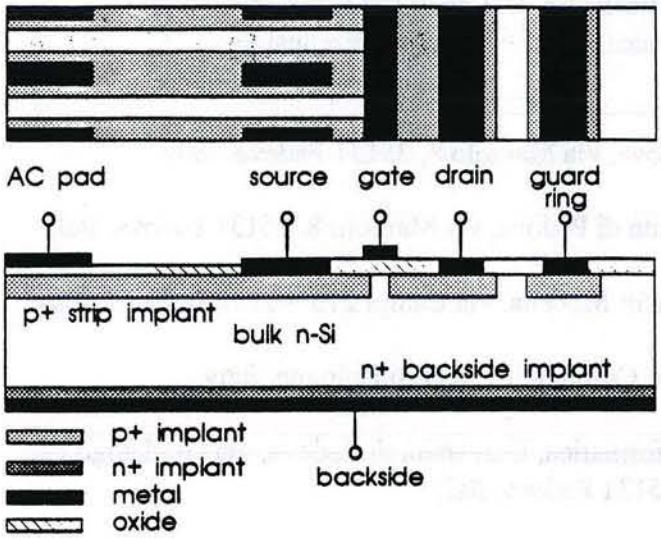

Fig.1 Schematic layout and cross-section of the microstrip detector in the FOXFET region (figure not in scale).

The DC electrical characteristics of detectors and test-patterns have been measured by using a computer driven HP4142B modular DC source/monitor and a microprobe station. Capacitance-voltage measurements have been taken by using a HP4284A LCR meter in the Rs-Cs mode, due to high series resistance of Si substrate. A HP4140B voltage source was used for external biasing and for quasistatic measurements. Both instruments were part of a computer-controlled measuring system.

In this study, Si detectors and test patterns have been irradiated with γ rays and protons without any external biasing.

Irradiations with γ rays were performed at room temperature by using two Co^{60} Nordion γ-cells with dose rates of 120 rad(Si)/s and 5 rad(Si)/s at the CNR-FRAE Institute, Bologna. The devices were inserted between two 3 mm thick polystyrene layers and placed in the middle of a cylindrical radiation field.

Proton irradiations were carried out at the CN Van der Graaff accelerator at the Laboratori Nazionali di Legnaro-INFN, Padova. Devices were irradiated in air: the proton beam crossed an aluminized mylar film window at the end of a vacuum line and was collimated on the device to irradiate homogeneously a 1 cm^2 square area. Irradiations over larger areas were performed in subsequent steps. The resulting energy of protons impinging the devices was 6 MeV.

Different radiation damage experiments were performed on various sets of samples: i) single step irradiation to a predetermined dose; ii) accumulation of radiation dose during subsequent irradiations. Time between subsequent irradiations was minimized to limit annealing phenome After each irradiation step, devices were measured within a fixed time interval (5 hours) and subsequently during a period of several months to detect room-temperature recovery effects. Devices were kept unbiased also during the long term storage.

III. Results and Discussion

A. FOXFET Biased Detectors

Before illustrating the experimental results, a short summary of the principles of operation of the FOXFET biased detectors is given in the following; a more detailed discussion could be found elsewhere [1, 2]. Basically, the long p^+ strips are biased through the p-channel FOXFET (see Fig.1): the p^+ drain contact, common to all strips, and the guard ring are grounded while the n^+ backside contact is positively biased. The gate voltage can be set to a desired value. This ensures reverse biasing of the p^+(strips)- n(substrate) strip diodes, which should be driven in full depletion for best charge collection.

In operating conditions, signals are collected at the AC pads and all strips (i.e., sources) are left floating. They automatically reach the voltage needed to drive the reverse current of the strip diodes to the grounded drain termi across the FOXFET channel. We have measured source voltage Vs as a function of the gate voltage Vg at fixed backside and drain voltages, Vb=30 V and Vd=0 V respectively, as shown in Fig. 2. As a conductive channel is formed due to the increase of the gate negative bias, the voltage Vs required to drive the strip diode reverse current across the FOXFET is lowered as well. The Vg value (Vgo) extrapolated at Vs=0 V allows to evaluate the gate bias corresponding to short-circuiting the source and drain contacts. Vs evaluated at Vg=0 V (Vso) indicates the strip self-bias in operating condition.

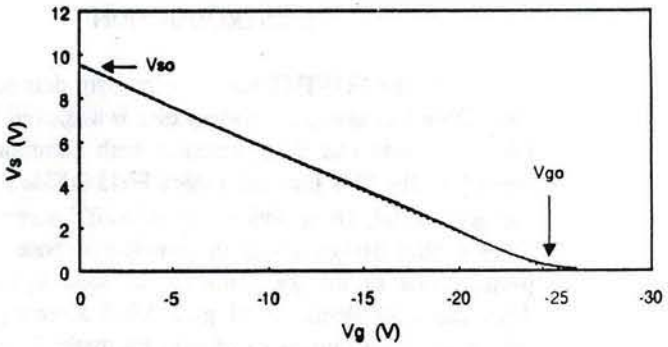

Fig.2 FOXFET source voltage Vs as a function of the gate voltage Vg measured at Vb=30 V, Vd=0 V.

The voltage difference Vb-Vso represents the reverse bias of the strip diodes, and therefore it determines the extension of the detector depleted region. Once Vso is known, which is determined in turn by the detector geometrical and

electrical properties, the Vb bias can be set to achieve the detector full depletion.

Given the low substrate doping, source and drain space charge regions already merge at zero bias, allowing for bulk punch-through conduction even before a surface conductive p-channel is established [1]. FOXFET electrical properties have been elucidated by using computer simulations [4]. The conductive channel between source and drain is formed below the Si surface, and extends toward the surface as the gate bias becomes more negative

Experimental results are grouped in two sections: 1) radiation effects; 2) room temperature annealing.

B. Radiation Effects

B.I Detector Leakage Current

Leakage current induced by radiation damage has been studied first of all on test pattern p^+-n diodes with guard-ring. After a 10 krad proton irradiation, the diode reverse current increases by a factor of 100, as shown in Fig.3. Correspondingly, the I-V forward characteristics show a pre-exponential factor increased approximately by the same factor. On the contrary, p^+-n junctions γ irradiated at the same 10 krad dose show negligible variations of the diode I-V characteristics (not shown).

In these p^+-n junctions, current is much more sensitive to the Si bulk properties than to surface effects. Hence, the different effects of γ and proton irradiations depend on the amount of bulk damage. Bulk damage, which is expected for proton irradiation, induces the creation of deep levels in the space charge region of the p^+-n diode [5]. Consequently, the hole lifetime in the bulk n-Si is reduced and the diode reverse current increases. Instead, the low level of lattice damage induced by γ rays leads only to negligible variations of the diode I-V curves.

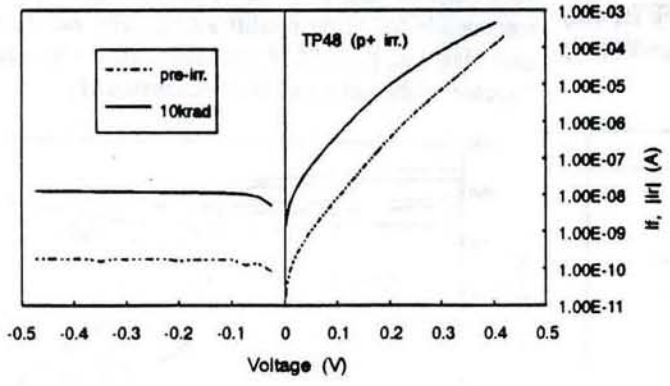

Fig.3 I-V characteristics of a p^+-n junction before and after a 10 krad proton irradiation.

One of the basic effects of ionizing particle irradiation on our detectors is the increase of the total leakage current Ib. Ib is measured at the backside contact by grounding gate, drain and guard ring and keeping all source floating, while the backside contact is reverse biased. Each strip approximately contributes the same current Is to the total current Ib, as measured grounding single strips through an ammeter, and Is≈Ib/(number of strips). The I_b increase with the Co^{60} cumulative γ dose can be observed in Fig.4, without any apparent saturation effect up to an integrated dose of 1 Mrad.

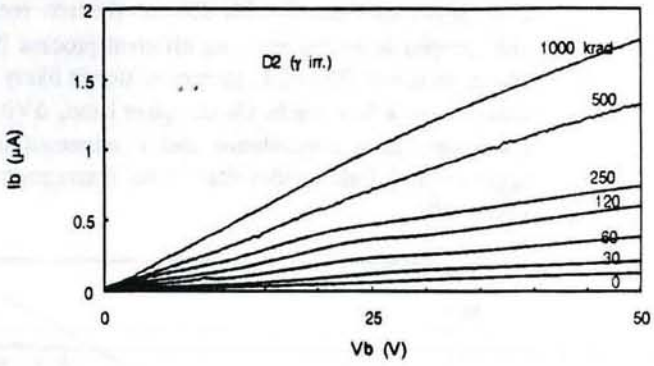

Fig.4 Total leakage current Ib of a γ irradiated detector at different cumulative doses.

An increase of Ib by a factor of 5 has been measured at Vb=30 V on a 30 krad proton irradiated detector, that is, similar to that measured after a much larger γ dose (120 krad). In general, the detector leakage current is higher after p^+ than after γ irradiations, for a fixed dose.

The leakage current variations in a proton irradiated detector are much less than in the test pattern p^+-n junctions. Moreover, the single strip leakage current Is is of the same order of magnitude of the diode reverse current, even though the test pattern diode p^+ region covers an area (1 cm^2) about 100 times larger than the strip. This indicates that the detector current Ib is controlled by the surface leakage contribution. According to previous literature data, Si/SiO_2 interface damage appears as the dominant origin of the Ib increase in γ irradiated detectors [6], while bulk damage contribution is not negligible after proton irradiation.

B.II FOXFET

Being an MOS device, the FOXFET is sensitive to radiation induced oxide charges. Fig.5 shows the variations of Vgo as a function of cumulative γ and p^+ doses. The Vgo growth follows the square root of dose, without any saturation effect in the dose range up to 1 Mrad. The growth rate is the same for both γ and p^+, on both detector and test pattern FOXFETs. Alternative evaluations of the FOXFET switching (threshold) voltage from the output characteristics of the device (i.e., source current vs. Vg), indicate the same growth rate, even though a much larger data dispersion is observed.

The Vgo variations upon irradiations derive from both accumulation of positive charge in the oxide layer and

formation of localized states at the Si/SiO_2 interface [7]. In irradiated MOSFETs the contributions of oxide charge (ΔVot) and interface states (ΔVit) to the threshold voltage shift ΔVt can be evaluated by analyzing the subthreshold output characteristics [8]. In FOXFETs this method is questionable due to the massive punch-through contribution to the output current and it is not possible to specify what is the dominant contribution to ΔVgo in Fig.5. Moreover, in MOS structures ΔVot grows sublinearly with dose as electron recombination with trapped holes becomes an efficient process [9]. In thick oxides, as in our FOXFET, such condition is likely established already after a few krads. On the other hand, ΔVit can follow a sublinear dose dependence and is expected to be much larger in thick field oxides than in the conventional thin gate oxides [10].

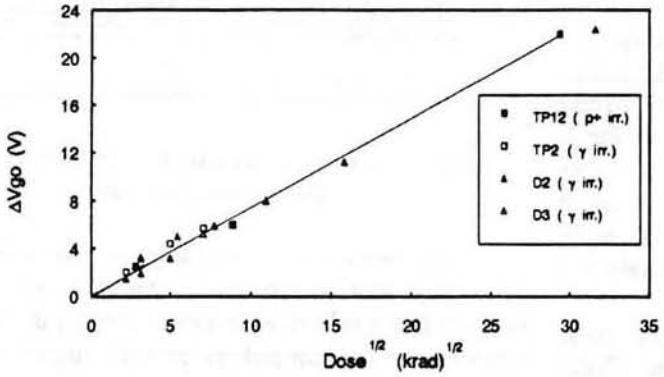

Fig.5 Variations of Vgo measured at Vb=30 V with γ and proton radiation dose.

After irradiation Vso is only slightly altered up to 1 Mrad as shown in Fig.6, while the FOXFET output current measured at Vs=Vso strongly increases with dose. This may seem contradictory with the increase of the FOXFET switching voltage with dose, but in this low current regime, corresponding to the subthreshold region in MOSFETs, only minor increments of Vso are sufficient to drive superlinearly growing currents to the drain [2].

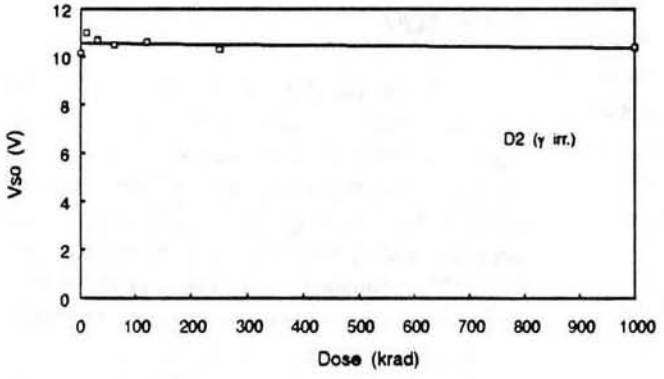

Fig.6 Variations of Vso measured at Vb=30 V with γ dose.

One well-known effect of ionizing radiation on MOSFETs is the degradation of subthreshold characteristics [11] due to build-up of Si/SiO_2 interface states. Even in FOXFET we have measured a slope decrease in the log(Is)-Vg curves at small |Vg| values with increasing γ dose, as reported in Fig.7.

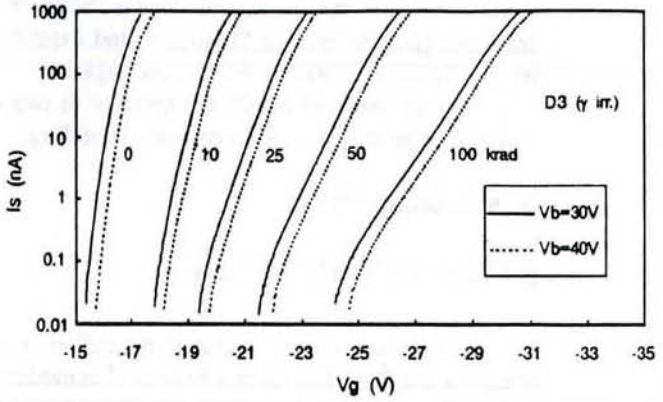

Fig.7 FOXFET subthreshold characteristics measured on a single strip at various γ doses.

Another fundamental detector parameter strongly affected by ionizing radiation exposure is the dynamic resistance Rd=dVs/dIs. In our devices Rd has been experimentally evaluated at various Vg values at Vb=30 V, Vs=0.1 V and Is=0 A, corresponding to the forecasted operational conditions in the CDF detector. Results are reported in Fig.8 for different γ doses.

The high-low abrupt transition of Rd which occurs at gate voltages between -22V and -26V in the unirradiated device, that is, around Vgo, corresponds to the onset of a conductive p-channel. After irradiation such transition is shifted to more negative Vg values and occurs also over an increasingly larger gate bias swing. As before, oxide charge accumulation and increase of the interface state density are responsible for these modifications. The Rd decrease at low gate bias, i.e., |Vg|<20 V, measured after irradiation is due to increase of the detectore leakage current [1].

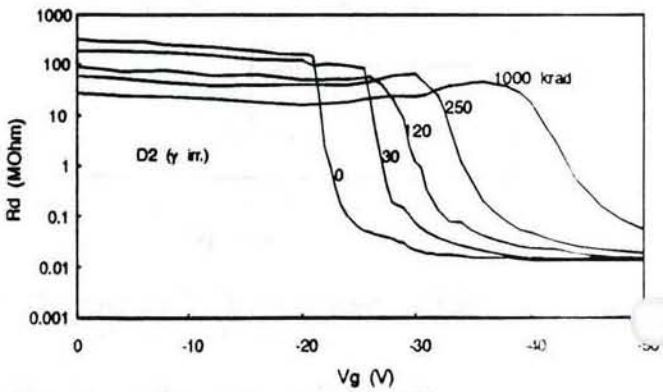

Fig.8 Detector dynamic resistance measured at Is=0, Vb=30 V, for different γ doses.

B.III MOS Capacitors

Radiation induced modifications of the FOXFET characteristics can be correlated to the results obtained on the test pattern MOS capacitors. Pre-irradiated capacitors show negligible hysteresis and frequency dispersion between 1 kHz and 300 kHz. Experimental and computed flat-band voltage deduced from C-V measurements agree within 0.5 V, indicating that the net positive charge induced in the oxide by the fabrication process is less than about 10^{10} cm^{-2}. Capacitance difference between accumulation and inversion corresponds to a doping level $Nd \approx 10^{12}$ cm^{-3} in agreement with the Si supplier specifications.

Capacitance-voltage curves obtained at 300 kHz for different γ doses are reported in Fig.9. At increasing γ doses C-V curves shift toward more negative voltages and stretchout grows, as expected [12].

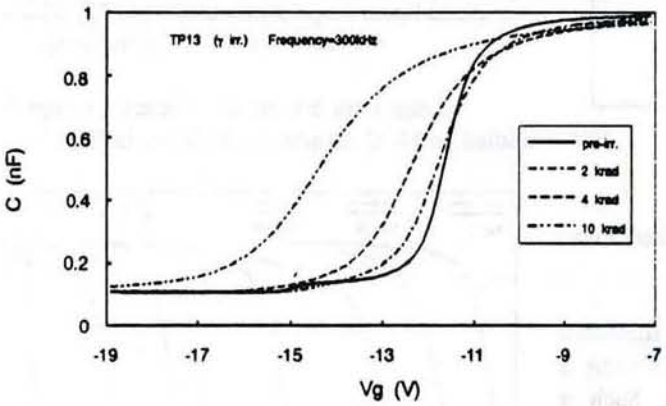

Fig.9 Degradation of the MOS C-V characteristics with γ dose.

Capacitance measurements after low dose γ irradiation have been elaborated to obtain interface trap density Dit and oxide trapped charge Qot.

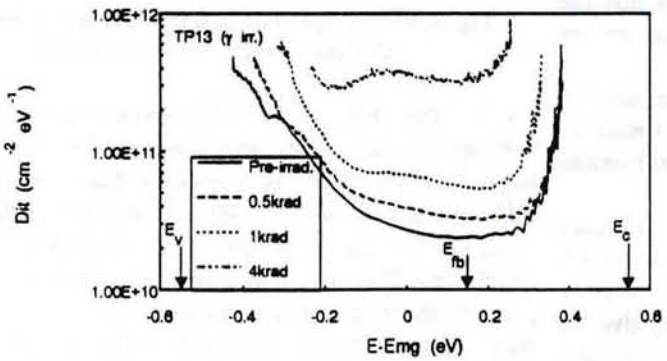

Fig.10 Density of interface states for γ irradiated MOS capacitor at different doses. Emg: midgap energy; Efb: flat-band energy.

The interface trap distribution has been evaluated by measuring the high frequency and quasi-static C-V curves with a ramp rate of 0.1V/s [13]. This method was chosen because nonuniform doping effects are cancelled out. The use of a 300 kHz signal for high frequency measurements was dictated by the high series resistance of the Si substrate, which made unreliable the usual 1 MHz curves. Typical Dit values are shown in Fig.10 for an MOS capacitor before and after low dose γ irradiations, i.e., when the quasi-static capacitance dip was clearly detectable and not largely deformed. The interface state density in pre-irradiated sample is continuous throughout the Si forbidden energy gap, with a U-shape monotonically increasing with energy toward the band edges from a minimum near midgap. The Dit curve is steeper above midgap: an asymmetrical Dit distribution is frequent for a <111> substrate [14]. After irradiation, Dit increases with dose and a broad peak gets visible, corresponding to a characteristic interface trap peak in the lower half of the Si band gap (Emg-0.05 eV) [15].

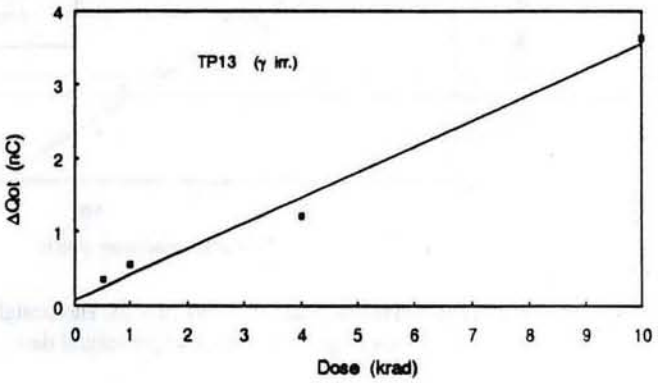

Fig.11 Positive charge trapped in SiO_2 at low γ doses.

The amount of positive trapped oxide charges ΔQot in irradiated MOS devices is shown in Fig.11, and it has been evaluated as [16]: $\Delta Qot = Cox * \Delta Vmg$, where Cox is the oxide capacitance and ΔVmg is the midgap capacitance voltage shift after irradiation in the high-frequency C-V curves. The conventional assumptions are made that: (a) nearly all of the radiation-induced oxide-trapped charge is located at the Si/SiO_2 interface; (b) interface states are neutral at midgap capacitance; (c) ΔVmg is determined primarily by hole trapping in the oxide.

As shown in Fig.11, ΔQot appears to linearly grow with dose, indicating that in this low dose range the electron-hole recombination process is not active [9]. The corresponding voltage shift ΔVmg closely follows the measured Vgo variations (see Fig.5), which hence must be attributed to oxide charge accumulation up to 10 krad.

C-V measurements performed at 100kHz apparently indicate a midgap voltage shift, ΔVmg, of about -70 V and midgap-to-flatband stretchout less than -20 V at 1 Mrad γ dose. Thus, 70-80% of the total radiation-induced shift in the C-V curve seems due to oxide-trap charge. However, for such a high dose the evaluation of Vmg becomes increasingly uncertain due to the interface state accumulation which contribute to the C-V curve shifts and frequency dispersion.

C. Room Temperature Annealing

Room temperature time decay of electrical characteristics of irradiated devices have been monitored during several months after irradiation; during the long term storage, the devices were kept unbiased. Devices selected for this study have been irradiated in a single step to the final dose of 1Mrad, to minimize the annealing effects occurring during sequential irradiations. Such effects could affect the results shown in paragraph 3.1, as no correction procedure was applied.

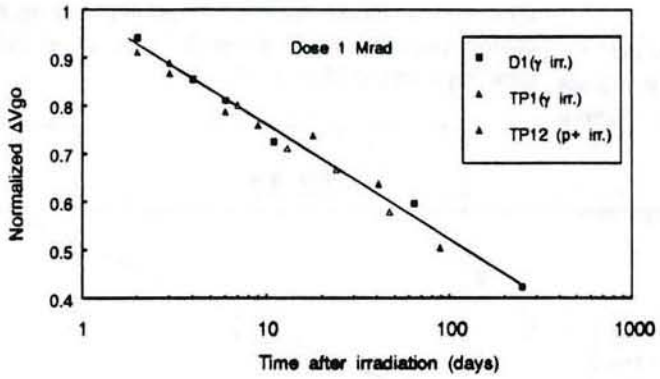

Fig. 12 Room temperature recovery of Vgo. The straight line is the least-squares fit of the experimental data.

Time variations of Vgo for γ and proton irradiated test patterns and devices are reported in Fig.12, showing a linear correlation between ΔVgo and log(time). Such a behaviour has been explained in terms of removal of holes trapped in the oxide near the Si/SiO_2 interface by thermally excited electrons, tunneling from the Si conduction band into the oxide [17]. As a consequence of the tunneling-recombination process, the annealing reproduces the spatial variation of the positive oxide charge distribution. The experimental linear dependence on log(t) indicates that the oxide trap density is uniform in space in the region we are sampling.

Relatively slow recovery occurs in these samples which indicates that the oxide charge distribution extends far into the bulk of oxide, which is characteristic for soft oxides [17].

Another detector parameter sensitive to room temperature long term annealing is the dynamic resistance Rd, as shown in Fig.13. The high-low transition voltage of the 1 Mrad single step irradiated detector shifts to less negative Vg values as a consequence of the annealing of the positive charges trapped in the oxide.

Instead, no recovery of the maximum value of Rd is observed. Rd is controlled by the detector total leakage current, which does not vary over a period of 4 months. Thus, no annealing of the generation-recombination centers responsible for the radiation induced increase of the leakage current can be expected at room temperature even over a long period. Such deep traps are located in bulk Si and, mainly, the Si/SiO_2 interface. The long term stability of these interface traps is confirmed by analyzing the "subthreshold" characteristics of the 1 MRad γ irradiated FOXFET, whose slope stays stable during several months after irradiation.

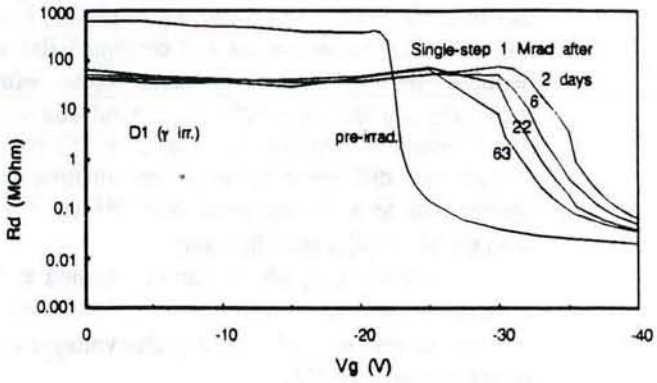

Fig.13 Room temperature annealing of FOXFET dynamic resistance after 1 Mrad γ irradiation.

Long term behaviour of interface traps has been also studied on MOS capacitors, as shown in Fig.14.

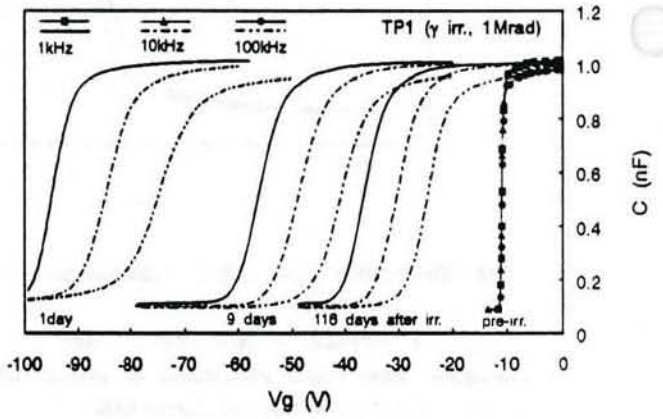

Fig.14 Room temperature modifications of high-frequency C-V curves after 1 Mrad γ irradiation.

The shift of the C-V curves toward less negative voltages is due to the annealing of the positive charges trapped in the oxide, as previously discussed. The midgap shift ΔVmg measured at 100 kHz changes with time from about -70 V (1 day after irradiation) to -20 V (116 days after irradiation). This should indicate that hole removal has taken place in an oxide region containing about 70% of the entire trapped holes. On the other hand, ΔVgo changes from -32 V to -12 V during the same period of time, i.e. much less than the shift of C-V curves. Such a discrepancy should attributed to an inexact evaluation of the midgap voltage, due to the interface state contribution at 100 kHz. C-V measurements at higher frequencies should be desirable to overcome this problem but are not routinely available on a high resistivity substrate.

As shown in Fig.14, while slight changes of the 1 kHz C-V curve shape are observed during room temperature storage, the 100 kHz curve becomes noticeably steeper as time is elapsed. Moreover, the frequency dispersion decreases after a 116 days storage. This behaviour could suggest a decrease of interface state density, but interface trap annealing is not expected at room temperature [18]. The observed effect could be attributed to annealing of lateral non uniformities in the oxide trapped charge [19], but in this case no frequency dependence should be observed [13]: Lateral non uniformities annealing could be responsible only for that part the time variations of the C-V curves common to all frequencies. We believe that the observed effect is due to an interface state redistribution over the forbidden gap, observed also in case of low dose irradiations [18].

IV. CONCLUSIONS

The main radiation damage effects after gamma or proton irradiation of FOXFET biased microstrip detectors consist of an increase of the total leakage current, while both the detector dynamic resistance and FOXFET switching voltage decrease. The switching voltage growth rate follows the dose square root, independently of the radiation source. Noticeably, no radiation induced variation of the strip self bias Vso is measured up to 1 Mrad γ dose.

The variations of the detector electrical parameters are mainly due to the generation of Si/SiO_2 interface traps and positive charge accumulation in the oxide film, as confirmed by C-V measurements on MOS capacitors. For proton irradiation, the increase of the detector leakage current can be supported also by bulk damage contribution.

A recovery of the pre-irradiation characteristics is seen only for the FOXFET switching voltage upon long term room temperature annealing, due to removal of oxide trapped holes. No annealing effects have been observed for electrical parameters controlled by the Si/SiO_2 interfacial states and bulk damage, such as leakage current and dynamic resistance.

These radiation tests, performed on unbiased devices, have identified the detector electrical parameters more sensitive to the radiation damage, showing that the most appealing operating region for our FOXFET-biased detectors lays at low |Vg| values, where Rd suffers tolerable modifications during irradiations.

V. ACKNOWLEDGEMENTS

The authors wish to thank L. Bosisio, S. Kashigin, C. Wilburn and A. Lucas for fruitful discussions and suggestions, and R. Cherubini and I. Motti for their valuable assistance during proton irradiations.

VI. REFERENCES

[1] P.P. Allport et al., "FOXFET Biassed Microstrip Detectors", *Nucl. Instr. Meth. A*, vol.A310, p.155, 1991.

[2] M. Laakso, P. Singh, E. Engels, Jr., and P.F. Shepard, "Operation and Radiation Resistance of a FOXFET Biasing Structure for Silicon Strip Detectors", *Nucl. Instr. Meth. A*, in press.

[3] N. Bacchetta, D. Bisello, G. Bolla, C. Canali, P.G. Fuochi, and A. Paccagnella, "Radiation Effects on AC-coupled Microstrip Detectors", *Nucl. Instr. Meth. A*, in press

[4] G. Verzellesi, unpublished data

[5] E.A. Burke, "Energy Dependence of Proton Induced Displacement Damage in Silicon", *IEEE Trans. Nucl. Sci.*, vol.NS-33, p.1276, 1986.

[6] A. Chilingarov, I. Dobnyo, S. Kurylo, and K. Trutzschler, "Radiation Damage of Silicon Microstrip Detectors by 1.5 MeV Electrons and Synchrotron Radiation", *Nucl. Instr. Meth. A*, vol.A310, p.277, 1991.

[7] H.E. Boesch and T.L. Taylor, "Charge and Interface State Generation in Field Oxide", *IEEE Trans. Nucl. Sci.*, vol.NS-31, p.1273, 1984.

[8] M. Gaitan and T.J. Russel, "Measurements of Radiation Induced Interface Traps Using MOSFETs", *IEEE Trans. Nucl. Sci.*, vol.NS-31, p.1256, 1984.

[9] H.E. Boesch and J.M. McGarrity, "Charge Yield and Dose Effects in MOS Capacitors", *IEEE Trans. Nucl. Sci.*, vol.NS-23, p.1520, 1976.

[10] T.P. Ma and P.V. Dressendorfer, *Ionizing radiation effects in MOS devices & circuits*, New York: J. Wiley & Sons, 1989, p.179.

[11] B.M. Baze, R.E. Plaag, and A.H. Johnston, "Dose Dependence of Interface Traps in Gate Oxides at High Levels of Total Dose", *IEEE Trans. Nucl. Sci.*, vol.NS-36, p.1858, 1989.

[12] K.G. Aubuchon, E. Harari, D.H. Leong, and C.P. Chang, "Effects of HCl Gettering, Cr Doping and Al Implantation on Hardened SiO", *IEEE Trans. Nucl. Sci.*, vol.NS-35, p.1192, 1988.

[13] E.H. Nicollian and J.R. Brews, *MOS Physics and Technology*, New York: J. Wiley & Sons, 1982, p.252.

[14] R.E Stahlbush, R.K.Lawrence, H.L. Hughes, and N.S. Saks, "Annealing of Total Dose Damage: Redistribution of Interface State Density on <100>, <110> and <111> Orientation Silicon", *IEEE Trans. Nucl. Sci.*, vol.NS-21, p.167, 1974.

[15] Yu Wang, T.P. Ma, and R.C. Barker, "Orientation Dependence of Interface-trap Transformation", *IEEE Trans. Nucl. Sci.*, vol.NS-36, p.1784, 1989.

[16] B.J. Mrstik, "Si-SiO_2 Interface State Generation During X-Ray Irradiation and During Post-Irradiation Exposure to a Hydrogen Ambient", *IEEE Trans. Nucl. Sci.*, vol.NS-38, p.1101, 1991

[17] A.J. Lelis, H.E. Boesch, T.R. Oldham, and F.B. McLean, "Reversibility of Trapped Hole Annealing", *IEEE Trans. Nucl. Sci.*, vol.NS-35, p.1186, 1988.

[18] R.E Stahlbush, B.J. Mrstik, and R.K. Lawrence, "Post-Irradiation Behaviour of the Interface State Density and the Trapped Positive Charge", *IEEE Trans. Nucl. Sci.*, vol.NS-37, p.1641, 1990.

[19] M.A. Xapsos, R.K. Freitag, C.M. Dozier, D.B. Brown, G.P. Sammers, E.A. Burke, and P.Shapiro. "Separation of Radiation Induced and Process Induced Lateral Nonuniformities", *IEEE Trans. Nucl. Sci.*, vol.NS-37, p.1677, 1990.